Volume 10
Number 41
7 November 2022
Pages 15211–15666

Journal of Materials Chemistry C

Materials for optical, magnetic and electronic devices

rsc.li/materials-c

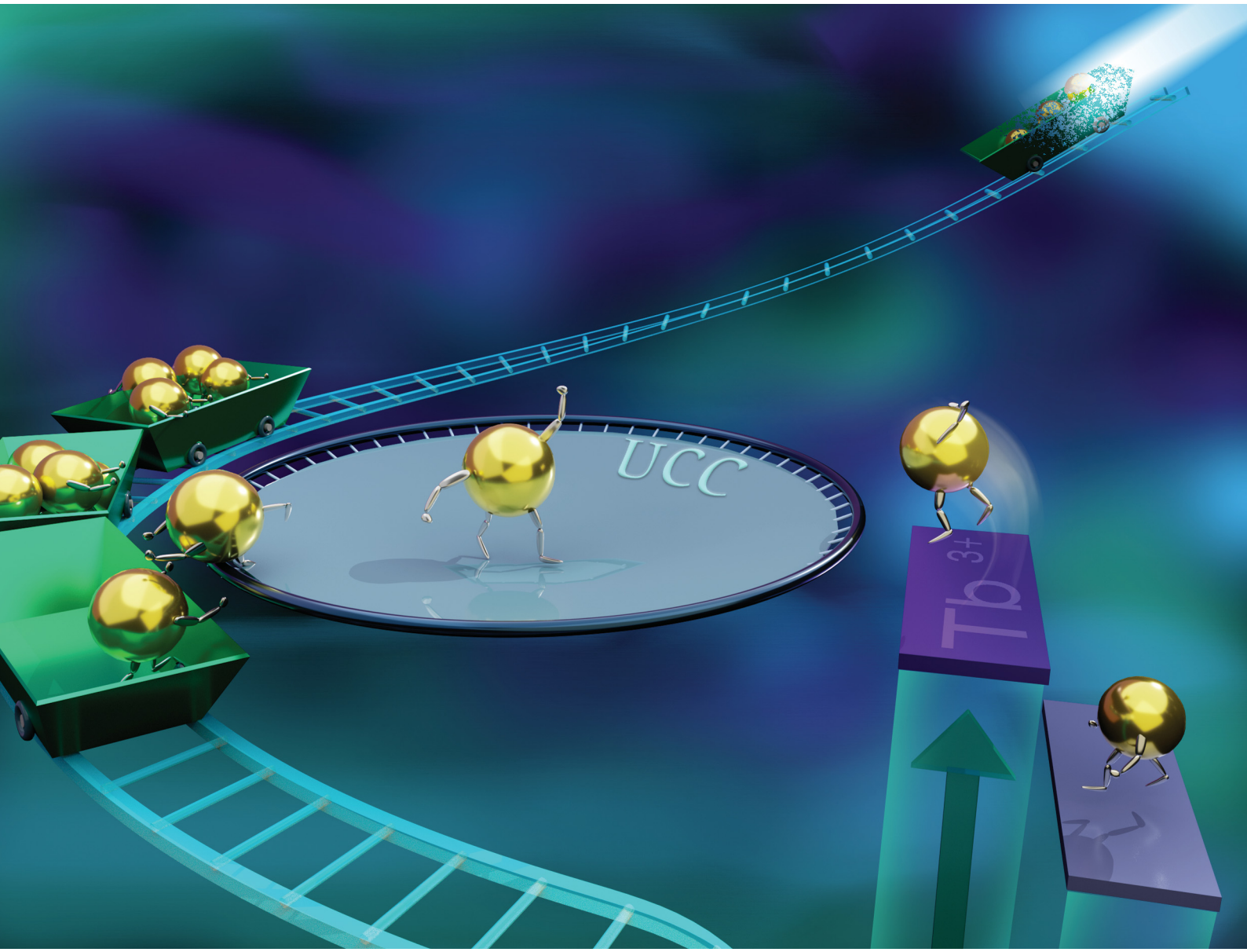

ISSN 2050-7526

ROYAL SOCIETY OF CHEMISTRY

PAPER

Feng Liu, Xiao-Jun Wang *et al.*

Up-conversion charging of a Tb^{3+}-activated garnet phosphor

Journal of Materials Chemistry C

ROYAL SOCIETY OF CHEMISTRY

PAPER

View Article Online
View Journal | View Issue

Cite this: J. Mater. Chem. C, 2022, 10, 15353

Up-conversion charging of a Tb^{3+}-activated garnet phosphor†

Tingxing Shi,[a] Feng Liu, *[a] Jiahua Zhang [b] and Xiao-Jun Wang *[c]

Received 11th August 2022,
Accepted 20th September 2022

DOI: 10.1039/d2tc03380a

rsc.li/materials-c

Studies on the up-conversion charging of persistent phosphors are of great academic and practical significance. To date, up-conversion charging designs have been achieved in Cr^{3+}, Mn^{2+} and Pr^{3+}-activated phosphors. We herein report, for the first time, an up-conversion charging process in the Tb^{3+}-activated garnet phosphor, $Gd_3Ga_5O_{12}$:Tb^{3+}, using a 488 nm laser as the excitation source. The delocalized $4f^7 5d$ state of Tb^{3+} is excited by absorbing two excitation photons, followed by the charging of the phosphor. Moreover, spectroscopic investigations reveal that an energy-transfer mechanism dominates the up-conversion excitation. This work provides an up-conversion strategy for charging Tb^{3+}-activated phosphors, paving the way toward expanding the scope of persistent phosphors with up-conversion chargeability.

Introduction

Trivalent terbium ion (Tb^{3+})-activated phosphors have been extensively investigated so far.[1–8] Much research has been devoted toward the search for Tb^{3+}-activated material systems as cathode-ray, X-ray and lamp phosphor systems.[9–13] The emission spectra of Tb^{3+} in phosphors feature sharp lines that have been assigned to $4f^8$ intra-configurational transitions, typically from the $^5D_4$ state ($^5D_4 \rightarrow {}^7F_J$).[14] Besides the reported steady-state luminescence measurements, persistent luminescence of Tb^{3+}-activated phosphors has also been well explored.[15–20] For instance, the Tb^{3+} may exhibit long-lasting emission in fluoride or oxide phosphors after X-ray irradiation. From an empirical viewpoint, people always take it for granted that the high-energy ionizing illumination is necessary for charging the persistent phosphors containing Tb^{3+} ions. However, this empirical view hinders the development of persistent luminescence. In recent years, studies of persistent phosphors chargeable by visible or infrared illumination have received considerable attention because the long-wavelength excitability holds promise for many promising applications ranging from afterglow bioimaging to "write/read" of optical information.[21–23]

Up-conversion charging (UCC) is an alternative approach for charging persistent phosphors upon visible or infrared illumination.[24–30] In a typical UCC process for phosphors, the electron traps are filled *via* a two-step ionization of the activator. So far UCC has been achieved in Cr^{3+}, Mn^{2+} and Pr^{3+}-activated phosphors.[23–30] According to the electronic structure and energy-level scheme, Tb^{3+} is also a potential activator ion for achieving the UCC process. In an appropriate phosphor, the Tb^{3+} ion has a tendency to oxidize and its $^5D_4$ state acts as an intermediate state to promote the up-conversion excitation process. Consequently, searching for appropriate phosphors containing Tb^{3+} with up-conversion chargeability is attractive but challenging.

In this work, we report the UCC performance of a Tb^{3+}-activated garnet phosphor, $Gd_3Ga_5O_{12}$:Tb^{3+}, using a 488 nm laser as the excitation source. The phosphor exhibits a long-lasting emission after a two-photon excitation and the associated ionization. We demonstrate that an energy-transfer up-conversion mechanism dominates the UCC in the phosphor. To the best of our knowledge, this is the first study of UCC in Tb^{3+}-activated phosphors.

Experimental

Materials synthesis

To validate the UCC process in the Tb^{3+}-activated phosphor, we designed and synthesized a series of garnet phosphors with a composition of $Gd_{3-x}Tb_xGa_5O_{12}$ (x = 0.01 − 0.4). The phosphors were synthesized *via* a usual solid-state approach and were confirmed to the pure garnet phase by X-ray diffraction measurements

[a] Key Laboratory for UV-Emitting Materials and Technology of Ministry of Education, Northeast Normal University, Changchun, 130024, China. E-mail: fengliu@nenu.edu.cn
[b] State Key Laboratory of Luminescence and Applications, Changchun Institute of Optics, Fine Mechanics and Physics, Chinese Academy of Sciences, Changchun, 130033, China
[c] Department of Physics, Georgia Southern University, Statesboro, GA, 30460, USA. E-mail: xwang@georgiasouthern.edu

† Electronic supplementary information (ESI) available: XRD patterns, persistent luminescence excitation spectrum, fluorescence decay curve, UCC upon illumination with a 375 nm laser, and UCC upon illumination by 488 and 532 nm lasers. See DOI: https://doi.org/10.1039/d2tc03380a

(Fig. S1, ESI†). Any dopant concentration of the phosphor composition can achieve UCC. Here we focus attention on a formula of $Gd_{2.7}Tb_{0.3}Ga_5O_{12}$, because among all the compositions we have prepared, it was the best one for the UCC performance. Stoichiometric amounts of Y_2O_3, Ga_2O_3 and Tb_4O_7 powders were mixed, finely ground, and then pressed under a 30-ton hydraulic pressure into pellets of 15 mm in diameter. Subsequently, the pellets were heated for 3 hours at 1330 °C in air to obtain the products.

Spectroscopic measurements

Emission and excitation spectra of the phosphor, as well as afterglow decay curves, were recorded at room temperature by a modular spectrofluorometer (QuantaMaster 8075-11, PTI), which was equipped with a CMOS detector (iStar-sCMOS-18U-73, Andor). Thermoluminescence curves were measured on a TL Reader (SL08-L, Rongfan) at a heating rate of 4 °C s^{-1}. The thermoluminescence measurement, as well as the afterglow decay, was conducted by monitoring the Tb^{3+} emission at 543 nm. Before each measurement, the phosphor was thermally bleached by heating it at 600 °C. The excitation sources applied in this work include a 488 nm laser diode, a 375 nm laser diode, a 532 nm solid-state laser, and a xenon arc lamp. In the present measurements, no optical heating with the phosphor was observed.

Results and discussion

Before the experimental demonstration of the UCC of $Gd_{2.7}Tb_{0.3}Ga_5O_{12}$, let us learn the conventional photoluminescence and persistent luminescence of the phosphor first. Fig. 1 shows the corresponding emission spectra, which share a similar spectral shape. Previous studies on Tb^{3+}-activated gallate phosphors have assigned the sharp-line emissions to intra-configurational

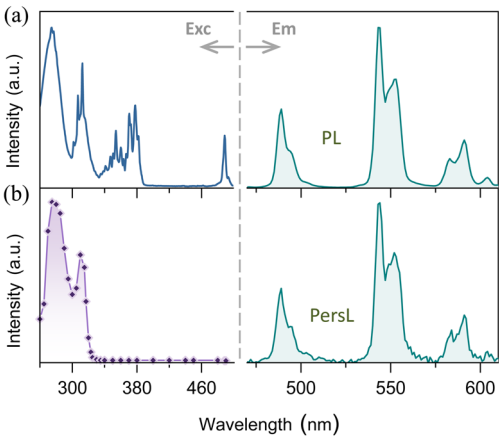

Fig. 1 Normalized emission and excitation spectra of $Gd_{2.7}Tb_{0.3}Ga_5O_{12}$ phosphor recorded at room temperature. (a) Steady-state photoluminescence (PL). Right-hand side: emission spectrum upon excitation at 275 nm. Left-hand side: excitation spectrum recorded by monitoring the 543 nm emission. (b) Conventional persistent luminescence (PersL). Right-hand side: emission spectrum recorded at 60 s after ceasing the 275 nm excitation. Left-hand side: excitation spectrum obtained by plotting the PersL emission intensity as a function of the excitation wavelength.

transitions of Tb^{3+}, consisting of the $^5D_4 \rightarrow {}^7F_6$ transition at 490 nm, $^5D_4 \rightarrow {}^7F_5$ transition at 540–550 nm, $^5D_4 \rightarrow {}^7F_4$ transition at 590 nm and $^5D_4 \rightarrow {}^7F_3$ transition at 620 nm.[14] Notably, for the Tb^{3+} concentration applied (x = 0.3 in $Gd_{3-x}Tb_xGa_5O_{12}$), emission from the $^5D_3$ state is absent.[31]

Fig. 1(a) (left-hand side) gives the photoluminescence excitation spectrum. It consists of characteristic excitation transitions of Tb^{3+}, involving sharp lines between 335 and 385 nm ($^7F_6 \rightarrow {}^5D_3/{}^5D_4$ transitions), a weak excitation band peak at 310 nm (spin-forbidden ($4f^8$) $^7F_6 \rightarrow 4f^7$5d transition) and an intense band peak at 275 nm (spin-allowed ($4f^8$) $^7F_6 \rightarrow 4f^7$5d transition).[32] Besides, in Fig. 1(a), we observe several sharp lines superimposed on the 310 nm excitation band. Such lines correspond to the excitation transitions within the $4f^7$ configuration of Gd^{3+}, indicating energy transfer from Gd^{3+} sublattice to Tb^{3+}.[32] Subsequently, we record the persistent luminescence excitation spectrum by plotting the afterglow emission intensity against the excitation wavelength (Fig. S2, ESI†). As shown in Fig. 1(b) (left-hand side), the persistent luminescence excitation spectrum covers ultraviolet region from 260 to 320 nm. The comparison between the two excitation spectra in Fig. 1 indicates that the onset of the electron delocalization energy (~320 nm) coincides with the onset of the spin-forbidden ($4f^8$) $^7F_6 \rightarrow 4f^7$5d excitation energy, revealing the delocalized character of the lowest $4f^7$5d excited state at room temperature.

Taking into account the energy of delocalized state in $Gd_{2.7}Tb_{0.3}Ga_5O_{12}$, the energy-level structure of Tb^{3+}, as well as the long lifetime of the $^5D_4$ state in the phosphor (2.52 ms, see Fig. S3, ESI†), a UCC process can be predicted. That is, upon an intense illumination with the appropriate wavelength, upconversion excitation of the Tb^{3+} electron into the delocalized $4f^7$5d state can occur, resulting in electron trapping, as illustrated in Fig. 2(a). Two approaches may be applied to charge the phosphor upon excitation into the Tb^{3+} $4f^8$ configuration. First, the $^5D_4$ state as the intermediate state may be directly populated under a 488 nm excitation, which fits well the 488 nm excitation peak [($4f^8$) $^7F_6 \rightarrow$ ($4f^8$) $^5D_4$ transition of Tb^{3+}] in the phosphor. Upon the intense excitation, the system may be further promoted from the intermediate state to the $4f^7$5d state, which is associated with electron delocalization at room temperature [Fig. 2(b)]. Second, upon excitation in the $^5D_3$ state using a 375 nm laser, the $^5D_4$ intermediate state may be fed by the $^5D_3$ state *via* a cross-relaxation process,[31] followed by the consequential promotion to the $4f^7$5d state. The traps in the phosphor may capture the delocalized electrons and then gradually release them at room temperature.

The conceptual UCC process in $Gd_{2.7}Tb_{0.3}Ga_5O_{12}$ has been experimentally demonstrated. Upon illumination with a 488 nm laser (power density, 1 W cm^{-2}), the phosphor exhibits UCC-induced persistent luminescence (UCC-PersL). Fig. 3(a) shows the UCC-PersL emission spectrum, which has a similar spectral shape to that of conventional photoluminescence. After ceasing the laser illumination, the corresponding UCC-PersL decay curve is recorded, as shown in the inset of Fig. 3(a). Although the UCC-PersL is detectable by the detector, the decayed emission intensity is too weak to be clearly observed by the naked eye in

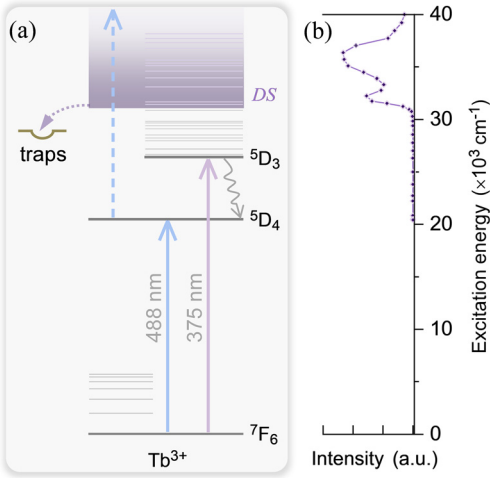

Fig. 2 (a) Schematic representation of the up-conversion charging (UCC) approach in $Gd_{2.7}Tb_{0.3}Ga_5O_{12}$ phosphor. Room-temperature delocalized state is indicated by DS (square frame region in shadow). (b) Persistent luminescence excitation spectrum, which is same as the one in Fig. 1(b), but in different coordinations.

the dark (the UCC-PersL luminance at 60 s delay is evaluated to be around 1.52 mcd m^{-2}).

To further understand the UCC mechanism of the $Gd_{2.7}Tb_{0.3}Ga_5O_{12}$ phosphor, extensive thermoluminescence spectroscopic investigation using a 488 nm laser is conducted, which may reveal the charging performance of the phosphor. We measure the thermoluminescence curves with different excitation parameters, including varied power densities (0.45–1.2 W cm^{-2}) but a fixed illumination duration of 10 s. The inset of Fig. 3(b) shows that these curves feature varied emission intensities but similar spectral shapes. A typical thermoluminescence curve is composed of two band peaks at 70 and 120 °C. Fig. 3(b) presents the thermoluminescence intensity (I) as a function of the laser power density (P). By fitting the plot, a quadratic dependence ($I \propto P^{1.91}$) is obtained, providing strong evidence that the trap in the phosphor is filled *via* a non-linear excitation.[28] Such a quadratic fit also implies that there is no saturation effect in the trapping/detrapping process upon illumination with the present doses.[29]

As pointed out above (Fig. 2), besides the 488 nm excitation, the UCC process of the $Gd_{2.7}Tb_{0.3}Ga_5O_{12}$ phosphor can be achieved upon 375 nm illumination. Such a UCC process has been demonstrated upon excitation with a 375 nm laser (0.4 W cm^{-2}). In this case, the Tb^{3+} ion is initially excited into the $^5D_3$ state, which undergoes nonradiative decay to the $^5D_4$ intermediate state, followed by a promotion into the Tb^{3+} $4f^7 5d$ state. The corresponding UCC-PersL and thermoluminescence data are presented in Fig. S4 (ESI†), in which the UCC-PersL performance agrees with the results presented in Fig. 3(a). The quadratic relationship between thermoluminescence intensity and the laser power density ($I \propto P^{1.56}$) indicates that the present UCC excitation involves two 375 nm excitation photons.

To gain insight into the UCC of the $Gd_{2.7}Tb_{0.3}Ga_5O_{12}$ phosphor, we study the mechanism that accounts for the up-conversion excitation. According to the typical up-conversion excitation mechanisms of phosphors,[33] after excitation in the $^5D_4$ intermediate state of Tb^{3+}, the system may be further promoted to the $4f^7 5d$ state by energy transfer or excited-state absorption. As a matter of fact, up-conversion in highly doped phosphor is often dominated by energy transfer mechanism, whereas the excited-state absorption mechanism often dominates up-conversion in a low-doped phosphor.[33] Accordingly, we prepare

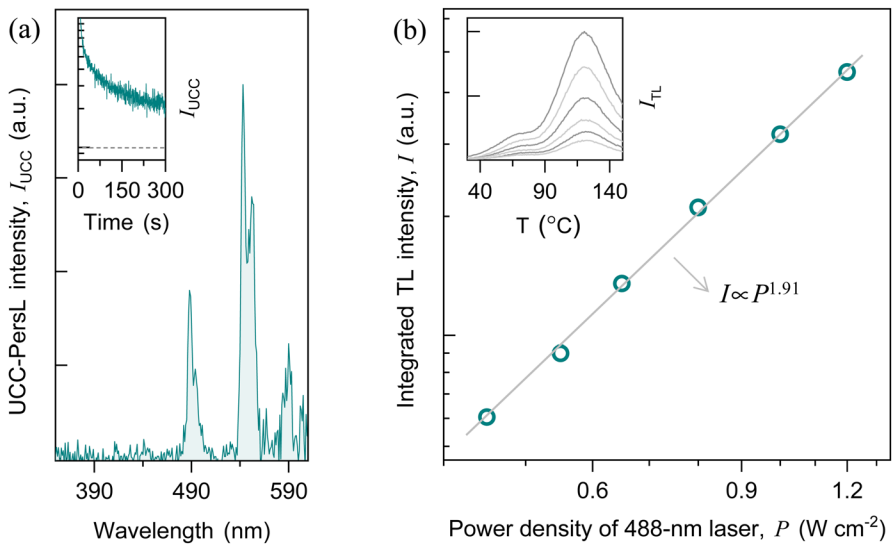

Fig. 3 Up-conversion charging-induced persistent luminescence (UCC-PersL) and thermoluminescence (TL) of $Gd_{2.7}Tb_{0.3}Ga_5O_{12}$ phosphor. (a) UCC-PersL emission spectrum recorded at 60 s after the end of 488 nm laser illumination (1 W cm^{-2} for 10 s). Inset shows the UCC-PersL decay curve, which is measured by monitoring the 543 nm afterglow emission. (b) Laser power density (P) *vs.* integrated TL intensity (I). The straight line is a quadratic fit of the data. Inset shows the corresponding TL curves, which are recorded after illuminating the phosphor for 10 s by the laser at different power densities (0.45–1.2 W cm^{-2}).

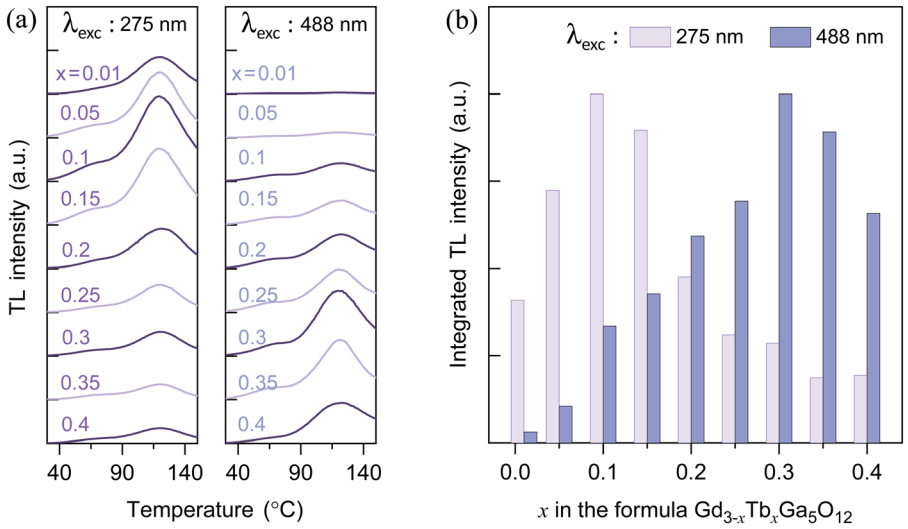

Fig. 4 (a) Thermoluminescence (TL) curves of the $Gd_{3-x}Tb_xGa_5O_{12}$ (x = 0.01 – 0.4) phosphors, which have been charged by 275 nm xenon light excitation (left-hand side) and by the 488 nm laser (right-hand side). (b) TL intensities recorded as a function of the Tb^{3+} content (x = 0.01 – 0.4). The comparison of the TL intensity dependence implies that an energy transfer up-conversion mechanism dominates the charging process upon illumination with the 488 nm laser.

samples with different Tb^{3+} contents, changing the value of x from 0.01 to 0.4 (here x is defined by the formula $Gd_{3-x}Tb_xGa_5O_{12}$). Firstly, we illuminate these phosphors under 275 nm ultraviolet excitation and record the thermoluminescence curves at different Tb^{3+} contents [left-hand side of Fig. 4(a)]. These curves exhibit a similar profile to that of the ones recorded after charging by the 488 nm laser. Fig. 4(b) shows that, upon 275 nm illumination, the thermoluminescence intensity reaches a maximum value for x = 0.1, and then decreases for higher Tb^{3+} concentrations due to concentration quenching. Subsequently, we use a 488 nm laser (1 W cm^{-2}) to excite each sample and record the thermoluminescence curves [right-hand side of Fig. 4(a)]. If an energy-transfer mechanism dominates the UCC excitation, a more efficient energy transfer is predictable along with a higher Tb^{3+} concentration. We plot the thermoluminescence intensity *versus* the Tb^{3+} content for the system $Gd_{3-x}Tb_xGa_5O_{12}$. Fig. 4(b) shows that, upon 488 nm illumination, the optimum content is at x = 0.3. Such a content results from a competition between the energy-transfer up-conversion and the concentration quenching of emission. The comparison of concentration dependence presented in Fig. 4 suggests that, upon the 488 nm laser illumination, the dominant mechanism for UCC excitation in $Gd_{2.7}Tb_{0.3}Ga_5O_{12}$ involves an energy-transfer step.

Although the energy-transfer is dominant for the UCC in the $Gd_{2.7}Tb_{0.3}Ga_5O_{12}$, it cannot be excluded that excited-state absorption contributes to the UCC. Subsequently, to testify the existence of the excited-state absorption, we use a combined excitation with the 488 and 532 nm laser to illuminate the phosphor (note that the 532 nm wavelength may be resonant with the ($4f^8$) $^5D_4 \rightarrow 4f^7 5d$ transition of Tb^{3+} but is out of resonance with the ground-state absorption transition). As shown in Fig. S5 (ESI†), upon the 488 nm illumination alone, as expected, the phosphor gives a distinct thermoluminescence signal while the thermoluminescence intensity is slightly enhanced after exposing the phosphor to the combined excitation (the 488 and 532 nm lasers). The small enhancement of thermoluminescence intensity results from the two-step excitation by the two lasers. From the above results, it can be concluded that the excited-state absorption process is involved in the present UCC process but is of no importance.

Conclusions

In summary, we have achieved, for the first time, a UCC process in a Tb^{3+}-activated phosphor, $Gd_{2.7}Tb_{0.3}Ga_5O_{12}$, which exhibits persistent luminescence after illumination with a 488 nm laser. The trap in the phosphor is filled *via* a non-linear excitation involving two excitation photons. The work outlines a fundamental principle to investigate the UCC of Tb^{3+}-activated phosphors. Future research could continue to expand the scope of phosphor systems with up-conversion chargeability.

Author contributions

F. L. conceived the experiments and was responsible for the project planning. T. S. synthesized the materials. T. S., J. Z., and X. W. carried out spectroscopic measurements. All of the authors discussed the results and contributed to the writing of the paper.

Conflicts of interest

There are no conflicts to declare.

Acknowledgements

This work was supported by the National Natural Science Foundation of China (11774046 and 11874055).

Notes and references

1 P. Vergeer, T. J. H. Vlugt, M. H. F. Kox, M. I. den Hertog, J. P. J. M. van der Eerden and A. Meijerink, *Phys. Rev. B: Condens. Matter Mater. Phys.*, 2005, **71**, 014119.
2 S. Guy, C. L. Bonner, D. P. Shepherd, D. C. Hanna, A. C. Tropper and B. Ferrand, *IEEE J. Quantum Electron.*, 1998, **34**, 900.
3 G. Blasse and A. Brill, *J. Chem. Phys.*, 1969, **51**, 3252.
4 J. M. Ogiegło, A. Zych, K. V. Ivanovskikh, T. Jüstel, C. R. Ronda and A. Meijerink, *J. Phys. Chem. A*, 2012, **116**, 8464.
5 B. Zhou, W. F. Yang, S. Y. Han, Q. Sun and X. G. Liu, *Adv. Mater.*, 2015, **27**, 6208.
6 C. He, Z. G. Xia and Q. L. Liu, *Opt. Mater.*, 2015, **42**, 11.
7 J. Zhou, Q. L. Liu and Z. G. Xia, *J. Mater. Chem. C*, 2018, **6**, 4371.
8 D. Wu, Y. Xiao, L. L. Zhang, X. L. Dong, S. F. Zhao, W. P. Zhou, Q. S. Lu and J. H. Zhang, *J. Mater. Chem. C*, 2020, **8**, 17176.
9 D. B. M. Klaassen, H. Mulder and C. R. Ronda, *Phys. Rev. B: Condens. Matter Mater. Phys.*, 1989, **39**, 42.
10 P. T. Mai, *J. Alloys Compd.*, 1995, **225**, 547.
11 A. Potdevin, G. Chadeyron, D. Boyer, B. Caillier and R. Mahiou, *J. Phys. D: Appl. Phys.*, 2005, **38**, 3251.
12 X. M. Liu and J. Lin, *J. Mater. Chem.*, 2008, **18**, 221.
13 S. Y. Wang, B. Devakumar, Q. Sun, J. Liang, L. L. Sun and X. Y. Huang, *J. Mater. Chem. C*, 2020, **8**, 4408.
14 G. Blasse and A. Bril, *Philips Res. Rep.*, 1967, **22**, 481.
15 D. Jia, R. S. Meltzer, W. M. Yen, W. Jia and X. Wang, *Appl. Phys. Lett.*, 2002, **80**, 1535.
16 J. Trojan-Piegza, J. Niittykoski, J. Hölsä and E. Zych, *Chem. Mater.*, 2008, **20**, 2252.
17 L. C. V. Rodrigues, H. F. Brito, J. Hölsä, R. Stefani, M. C. F. C. Felinto, M. Lastusaari, T. Laamanen and L. A. O. Nunes, *J. Phys. Chem. C*, 2012, **116**, 11232.
18 J. S. Zhang, Z. D. Hao, X. Zhang, Y. S. Luo, X. G. Ren, X. J. Wang and J. H. Zhang, *J. Appl. Phys.*, 2009, **106**, 034915.
19 D. Van der Heggen, D. R. Cooper, M. Tesson, J. J. Joos, J. Seuntjens, J. A. Capobianco and P. F. Smet, *Nanomaterials*, 2019, **9**, 1127.
20 X. Y. Ou, X. Qin, B. L. Huang, J. Zan, Q. X. Wu, Z. Z. Hong, L. L. Xie, H. Y. Bian, Z. G. Yi, X. F. Chen, Y. M. Wu, X. R. Song, J. Li, Q. S. Chen, H. H. Yang and X. G. Liu, *Nature*, 2021, **590**, 410.
21 Z. W. Pan, Y. Y. Lu and F. Liu, *Nat. Mater.*, 2012, **11**, 58.
22 F. Liu, W. Z. Yan, Y. J. Chuang, Z. P. Zhen, J. Xie and Z. W. Pan, *Sci. Rep.*, 2013, **3**, 1554.
23 Q. Q. Gao, C. L. Li, Y. C. Liu, J. H. Zhang, X. J. Wang and F. Liu, *J. Mater. Chem. C*, 2020, **8**, 6988.
24 F. Liu, Y. J. Liang and Z. W. Pan, *Phys. Rev. Lett.*, 2014, **113**, 177401.
25 F. Liu, Y. F. Chen, Y. J. Liang and Z. W. Pan, *Opt. Lett.*, 2016, **41**, 954.
26 Y. F. Chen, F. Liu, Y. J. Liang, X. L. Wang, J. Q. Bi, X. J. Wang and Z. W. Pan, *J. Mater. Chem. C*, 2018, **6**, 8003.
27 S. Y. Yan, F. Liu, J. H. Zhang, X. J. Wang and Y. C. Liu, *Phys. Rev. Appl.*, 2020, **13**, 044051.
28 S. Y. Yan, Q. Q. Gao, X. Y. Zhao, A. Y. Wang, Y. C. Liu, J. H. Zhang, X. J. Wang and F. Liu, *J. Lumin.*, 2020, **226**, 117427.
29 X. Y. Zhao, C. L. Li, F. Liu and X. J. Wang, *J. Rare Earths*, 2021, **39**, 1492.
30 C. L. Li, X. Y. Zhao, T. Guo, F. Liu, X. J. Wang, C. Liao and J. H. Zhang, *Acta Phys. Sin.*, 2022, **71**, 077801.
31 Z. Boruc, B. Fetlinski, M. Kaczkan, S. Turczynski, D. Pawlak and M. Malinowski, *J. Alloys Compd.*, 2012, **532**, 92.
32 M. J. J. Lammers, J. W. Severin and G. Blasse, *J. Electrochem. Soc.*, 1987, **134**, 2356.
33 F. Auzel, *Chem. Rev.*, 2004, **104**, 139.